ОБЪЕДИНЕННЫЙ
ИНСТИТУТ
ЯДЕРНЫХ
ИССЛЕДОВАНИЙ
ДУБНА

E1-91-496

THE DIFFERENTIAL CROSS SECTIONS FOR INCLUSIVE REACTIONS $\pi^{+} + A \rightarrow \eta + X$ AT 10 GeV

Submitted to "Nuclear Physics B"

1991

1. Introduction

The space dimensions of the region in which quarks behave as quasi-free objects increase with the interaction energy. At the energies of tens of GeV they are already comparable with the size of atomic nuclei (e.g. see Ref.[1]). So the investigation of hadron-nucleus interactions allows a unique possibility of studying the properties of the intermediate quark-parton structure as a result of its "re-scattering" on intranuclear nucleons.

A large program for investigations of the hadron-nucleus interactions at energy of 10 GeV has been carried out [2-5] by HYPERON collaboration at the Serpukhov accelerator. In this paper our results for inclusive reactions

$$\pi^{+} + A \longrightarrow \eta + X \qquad (1)$$

(A=H,D,Li,Be,Al,Cu)at the beam energy of 10.5 GeV are presented. The kinematic region covered corresponds to the fragmentation of the beam particle:

$$0{,}60 \le x_F \le 1.0; \qquad 0 \le p_t^2 \le 0.6\ (\mathrm{GeV}/c.)^2.$$

The reaction with an η-meson in the final state has been chosen because practically all η-mesons in this energy region are produced in the primary act, i.e. the yield of η-mesons from decays of heavier resonances, which could distort the picture, is negligible. This facilitates the theoretical analysis of the processes studied. Fragmentation of pions into η-mesons on atomic nuclei has been experimentally studied in our earlier papers [3-5] based on lower statistics.

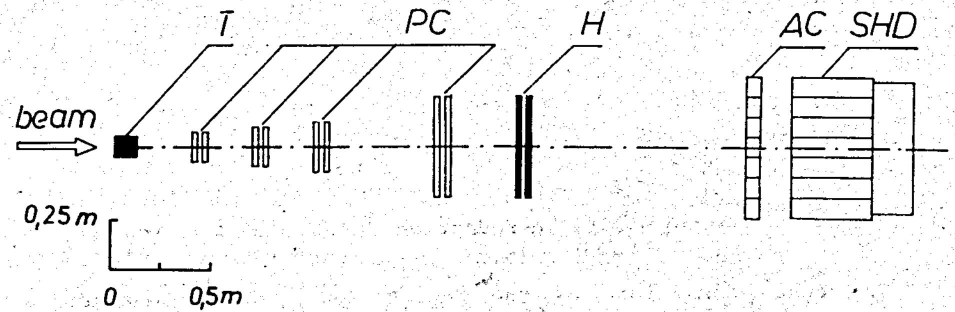

Fig. 1. Experimental facility

2. Differential cross sections for production of η-mesons by pions on a nucleon and nuclei

Measurements have been carried out at the HYPERON spectrometer [6,7] situated in the beam of positive particles with the momentum 10.5 GeV/c at the Serpukhov accelerator. The η-mesons have been registered by their decay into two γ-quanta. The gammas have been detected by the multichannel Cherenkov shower hodoscopic detector (SHD) with an active converter (AC), both made of lead glass (see Fig.1). Proportional chambers PC and scintillation hodoscope H have been used to reconstruct the tracks of charged particles. The setup, experimental conditions and data processing was described in detail in Ref. [4,5,7-9].

During the run $3.4 \cdot 10^9$ π^+-mesons passed through the facility. The total amount of $5 \cdot 10^4$ η-mesons have been detected. A γ-quanta pairs invariant mass spectrum, obtained in one of the x_F-intervals and corrected for geometrical acceptance of the apparatus and trigger efficiency, is shown in Fig.2.

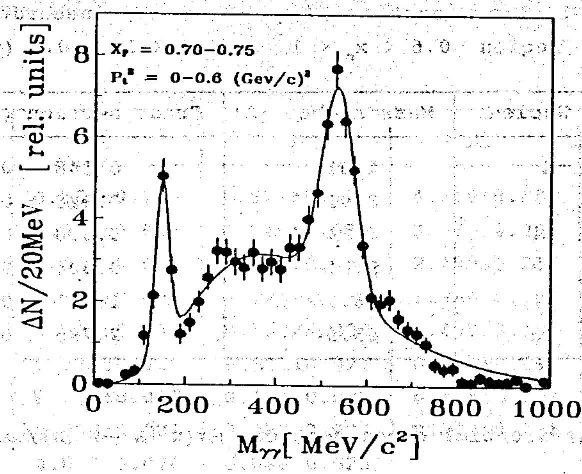

Fig. 2. An example of acceptance corrected events distribution over the invariant mass of $\gamma\gamma$ pairs in the reaction $\pi^+ + D \to \gamma\gamma + X$. Detection of $\gamma\gamma$ pairs with a mass < 400 MeV/c^2 is suppressed by special trigger condition applied [4,8]

The measured integral inclusive cross sections

$$\Delta\sigma\ (\pi^+ + A \to \eta + X) = \int dx_F \int dp_t^2 \frac{d^2\sigma\ (\pi^+ + A \to \eta + X)}{dp_t^2\ dx_F} \qquad (2)$$

$$0.60 \le x_F \le 1.0; \quad 0 \le p_t^2 \le 0.6\ (\mathrm{GeV/c})^2 .$$

are presented in Table 1 and Fig.3. The errors have been determined in the fitting procedure MINUIT [10]. We estimate the systematic errors of the cross sections to be as large as (-5%,+20%). These errors are mainly due to ambiguity in choosing the form of the non-resonance background in distributions like the one in Fig. 2.

Table 1. Cross sections $\Delta\sigma(\pi^{+}+A \longrightarrow \eta X)$ integrated over the region $0.6 < x_F < 1$ and $0 < P_t^2 < 0.6$ $(GeV/c)^2$.

Nucleus	Mass number (A)	Cross section (millibarns)
H	1.01	0.148 ± 0,009
D	2.01	0.328 ± 0.011
Li	6.94	0.860 ± 0.036
Be	9.01	0.904 ± 0.060
Al	26.98	1.711 ± 0.155
Cu	63.54	2.795 ± 0.309

Table 2. Differential cross sections $d\sigma(\pi^{+}+A \longrightarrow \eta X)/dx_F$ (mb/unit).

x_F	H	D	Li
0.625	0.774±0.150	1.750±0.260	3.980±0.920
0.675	0.759±0.053	1.540±0.060	4.130±0.510
0.725	0.580±0.056	1.120±0.090	3.600±0.270
0.775	0.421±0.029	0.896±0.046	2.500±0.230
0.825	0.262±0.042	0.800±0.047	2.120±0.190
0.875	0.202±0.023	0.567±0.037	1.686±0.139
0.925	0.021±0.015	0.260±0.031	1.044±0.115
0.975	0.009±0.009	0.086±0.012	0.325±0.105

x_F	Be	Al	Cu
0.625	4.450±1.410	8.950 3.200	14.160±5.130
0.675	4.610±0.590	8.690±1.270	12.510±2.140
0.725	3.950±0.300	7.060±0.600	10.490±1.160
0.775	2.850±0.220	5.310±0.450	7.830±0.880
0.825	2.080±0.140	3.850±0.350	7.370±0.690
0.875	1.600±0.120	2.440±0.300	4.520±0.500
0.925	1.038±0.108	1.560±0.260	3.020±0.490
0.975	0.371±0.089	0.460±0.200	1.160±0.410

Table 3. Differential cross sections $d\sigma(\pi^{+}+A \longrightarrow \eta X)/dp_t^2$ $(mb/(GeV/c)^2)$.

p_t^2	H	D	Li
0.025	0.563±0.100	0.922±0.105	4.610±0.680
0.075	0.508±0.057	1.240±0.078	3.930±0.290
0.125	0.441±0.048	0.885±0.061	2.470±0.210
0.175	0.353±0.050	0.794±0.073	1.900±0.190
0.250	0.200±0.031	0.536±0.033	1.450±0.104
0.350	0.144±0.025	0.313±0.027	0.604±0.091
0.450	0.030±0.016	0.161±0.027	0.375±0.065
0.550	0.052±0.021	0.059±0.029	0.214±0.168
0.700	0.011±0.020	0.048 0.025	

p_t^2	Be	Al	Cu
0.025	5.230±0.840	7.900±1.390	15.710±2.460
0.075	3.910±0.310	6.680±0.640	9.280±1.130
0.125	2.380±0.200	4.380±0.420	6.950±0.730
0.175	2.000±0.180	3.530±0.440	6.460±0.760
0.250	1.680±0.110	2.940±0.260	4.330±0.470
0.350	0.777±0.112	1.470±0.270	2.540±0.470
0.450	0.498±0.113	0.985±0.092	2.710±0.630
0.550	0.336±0.335	1.080±0.950	1.700±1.700

The curve in Fig. 3 represents the power dependence of cross section $\Delta\sigma$ on the mass number A of the target nucleus:

$$\Delta\sigma = \Delta\sigma_0 \cdot A^{\alpha} . \tag{3}$$

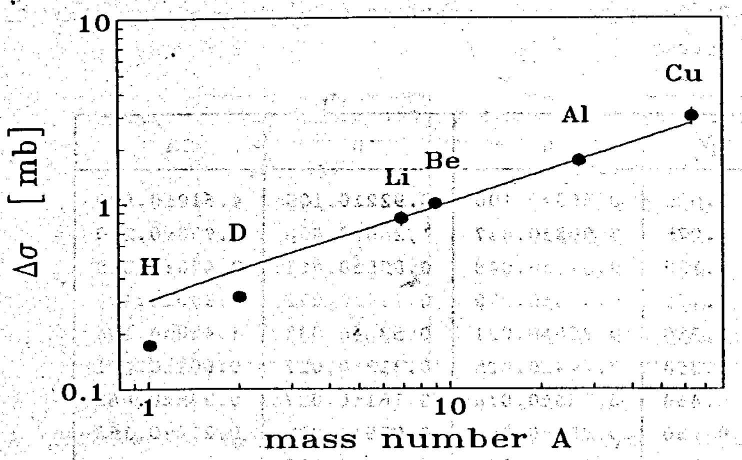

Fig. 3. The integrated cross section for process $\pi^{+}+A\longrightarrow\eta+X$ vs target nucleus mass number. The curve is the result of fit by function (3) (see text)

The cross sections on Li, Be, Al, Cu nuclei have been used to obtain the following values of the parameters:

$$\Delta\sigma = 0.299 \pm 0.029 \text{ mb}, \ \alpha = 0.532 \pm 0.035.$$

The measured differential cross sections

$$\frac{d\sigma}{dx_F}(\pi^{+}+A \longrightarrow \eta+X) = \int dp_t^2 \ \frac{d^2\sigma \ (\pi^{+}+A \longrightarrow \eta+X)}{dp_t^2 \ dx_F}$$

and

$$\frac{d\sigma}{dp_t^2}(\pi^{+}+A \longrightarrow \eta+X) = \int dx_F \ \frac{d^2\sigma \ (\pi^{+}+A \longrightarrow \eta+X)}{dp_t^2 \ dx_F},$$

where A = H,D,Li,Be,Al,Cu, are shown in tables 2,3 and Fig. 4,5.

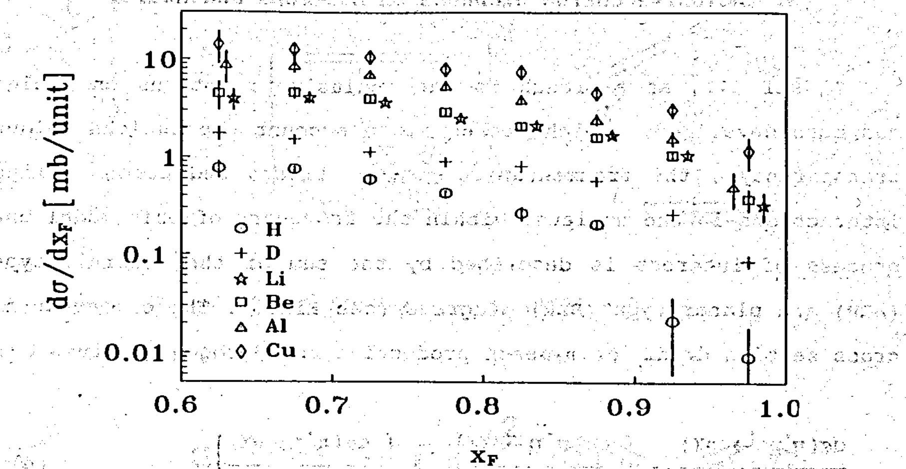

Fig.4. Differential cross sections $d\sigma/dx_F$ for process $\pi^{+}+A\longrightarrow\eta+X$ on the targets H,D,Li,Be,Al,Cu

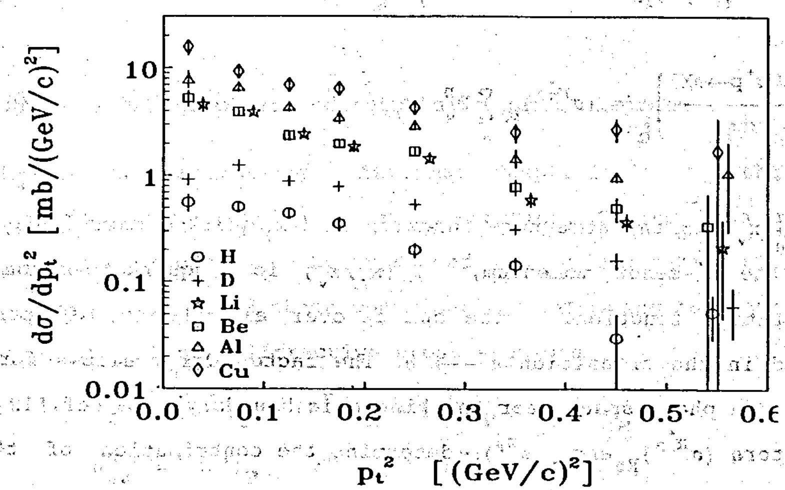

Fig.5. Differential cross sections $d\sigma/dp_t^2$ for process $^{+}+A\longrightarrow\eta+X$ on the targets H,D,Li,Be,Al,Cu

3. Inclusive charge exchange on nucleons and nuclei

In Ref [11] an approach to the inclusive reactions on nuclei has been developed, which takes into account the nucleus colour transparency , the fragmentation length effects and colour string interactions in the nucleus. Within the framework of this model the process of interest is described by the sum of the cylinder-type (**RRP**) and planar-type (**RRR**) diagrams (see Fig.6). The differential cross section $d\sigma/dx_F$ of η-meson production on hydrogen is given by:

$$\frac{d\sigma(\pi^+p\rightarrow\eta X)}{dx_F} = \left(\frac{d\sigma(\pi^+p\rightarrow\eta X)}{dx_F}\right)_{\mathbf{P}} + \left(\frac{d\sigma(\pi^+p\rightarrow\eta X)}{dx_F}\right)_{\mathbf{R}}, \quad (4)$$

$$\left(\frac{d\sigma(\pi^+p\rightarrow\eta X)}{dx_F}\right)_{\mathbf{P}} = \Omega(x_F)\cdot(\sigma^{\pi p})_{\mathbf{P}} \sum_q \int_x^1 \frac{dx_v}{x_v} F^q_{\pi^+}(x_v)\, D^\eta_q(x_F/x_v), \quad (5)$$

$$\left(\frac{d\sigma(\pi^+p\rightarrow\eta X)}{dx_F}\right)_{\mathbf{R}} = (\sigma^{\pi^+p})_{\mathbf{R}} \sum_q D^\eta_q\,(x_F)\ . \quad (6)$$

Here $F^q_{\pi^+}(x_v)$ is the structure function of the quark q carrying part x_v of the π^+-meson momentum, $D^\eta_q(x_F/x_v)$ is a quark-to-meson η fragmentation function*. The sum is over all flavors of quarks involved in the transition $\pi^+\longrightarrow\eta$. The factor $\Omega(x_F)$ allows for a decrease in phase space near the kinematic boundary (see Ref.[12]). The factors $(\sigma^{\pi^+p})_{\mathbf{R}}$ and $(\sigma^{\pi p})_{\mathbf{P}}$ determine the contribution of the

---

* As $D^\eta_q(x_F/x_v)$ we have used the π-meson fragmentation function $D^\pi_q(x_F/x_v)$ in assumption of small contribution of strange quarks.

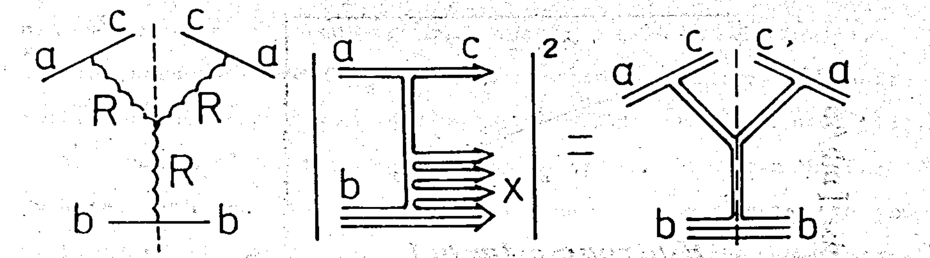

Fig.6a. **RRR** graph and corresponding quark diagrams

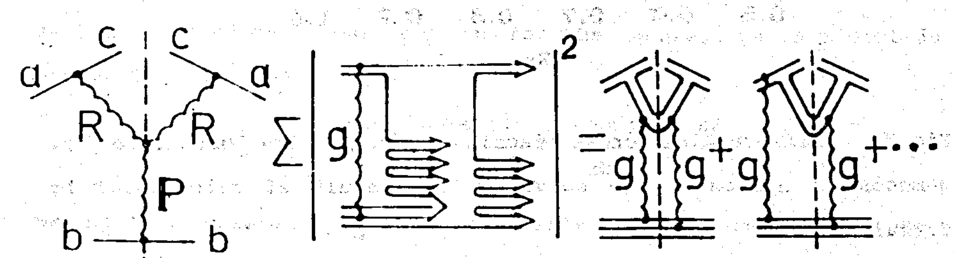

Fig.6b. **RRP** graph and corresponding quark diagrams

cylinder- and planar-type diagrams respectively to the non-diffraction cross section of πN-interaction. Taking into account the fact that reggeon can be expressed as a superposition of ρ- and f-mesons, we can find these contributions comparing the experimental π^+N- and π^-N non-diffractive cross sections:

$$\sigma^{\pi^+p}_{nd} = (\sigma^{\pi p})_{\mathbf{P}} + (\sigma^{\pi^+p})_{\mathbf{R}} = (\sigma^{\pi p})_{\mathbf{P}} + \sigma_{\mathbf{f}} - \sigma_\rho$$
$$\sigma^{\pi^-p}_{nd} = (\sigma^{\pi p})_{\mathbf{P}} + (\sigma^{\pi^-p})_{\mathbf{R}} = (\sigma^{\pi p})_{\mathbf{P}} + \sigma_{\mathbf{f}} + \sigma_\rho.$$

Using $\sigma_{\mathbf{f}} = 4{,}8\cdot(\sigma^{\pi p})_{\mathbf{P}}\cdot s^{-0.6}$ from Ref [14] we obtained $(\sigma^{\pi p})_{\mathbf{P}}$=10 mb

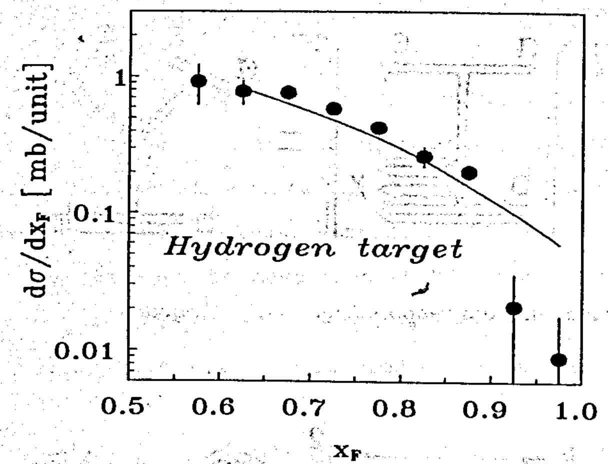

Fig.7. Differential cross section $d\sigma/dx_F$ for production of η-meson on hydrogen. The curve is the result of calculation by formula (4)

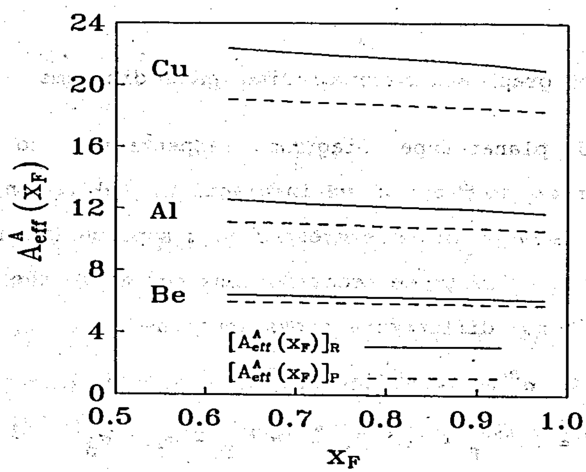

Fig.8. The effective number of nucleons in a nuclei $A^A_{eff}(x_F)$ for the targets Be,Al,Cu

and $(\sigma^{\pi^+p})_R$ = 6.8 mb at our energy (s = 20.6 (GeV)²).

The structure and fragmentation functions obtained in the framework of the quark-gluon string model (QGSM) have been used [13].

The result of calculation of $d\sigma(\pi^+p\to\eta X)/dx_F$ is shown on fig. 7 together with the experimental data. One can see that the predictions of the model are in good agreement with the experimental data.

Now we turn to consider the cross section $d\sigma/dx_F$ of process (1) on nucleus. We define the effective number of nucleons in a nuclei as the ratio of the cross sections for the interaction on a nucleus and on free nucleon:

$$A^A_{eff}(x_F) = \frac{d\sigma(\pi^+A \longrightarrow \eta X)}{dx_F} / \frac{d\sigma(\pi^+p \longrightarrow \eta X)}{dx_F}$$

We have calculated $A^A_{eff}(x_F)$ for different targets within the framework of model used [11]. The results are shown in fig.8. Then the differential cross section $d\sigma/dx_F$ of the process $\pi^+A\to\eta X$ is given by:

$$\frac{d\sigma(\pi^+A \to \eta X)}{dx_F} = \left(\frac{d\sigma(\pi^+p\to\eta X)}{dx_F}\right)_P \cdot \left(A^A_{eff}(x_F)\right)_P + \left(\frac{d\sigma(\pi^+p\to\eta X)}{dx_F}\right)_R \cdot \left(A^A_{eff}(x_F)\right)_R \quad (7)$$

The calculations by formula (7) for different targets are presented in fig. 9.

To describe the p_t^2-dependence of the cross section of η-meson inclusive production on hydrogen we have used the following parameterization of expressions (5) and (6):

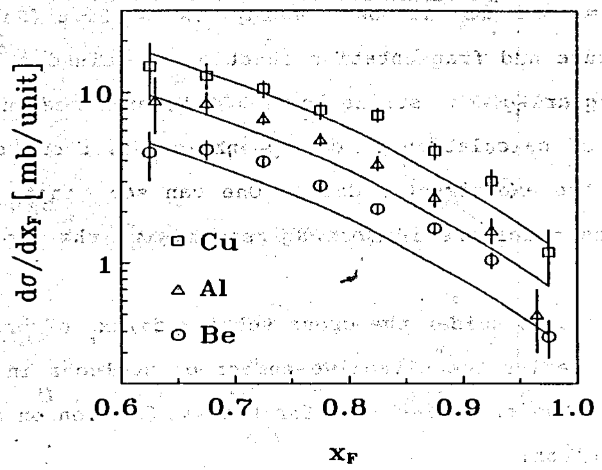

Fig.9. Differential cross sections $d\sigma/dx_F$ for process $\pi^+ + A \longrightarrow \eta + X$ on the targets Be,Al,Cu. The curve is the result of calculation by formula (7)

$$\frac{d\sigma(\pi^+ p \longrightarrow \eta X)}{dp_t^2} = \int B_P \cdot \exp(-B_P \cdot p_t^2) \cdot \left(\frac{d\sigma(\pi^+ p \longrightarrow \eta x)}{dx_F}\right)_P dx_F + \int B_R \cdot \exp(-B_R \cdot p_t^2) \cdot \left(\frac{d\sigma(\pi^+ p \longrightarrow \eta x)}{dx}\right) dx_F , \qquad (8)$$

where $B_P = B_P^o - 2\alpha'_{A_2} \cdot \ln(1-x_F)$, $B_R = B_R^o - 2\alpha'_{A_2} \cdot \ln(1-x_F)$, α'_{A_2} is the slope parameter of Regge-trajectories, B_P^o and B_R^o are free parameters. At high energies and $x_F \longrightarrow 1$ the cylinder-type diagram corresponds to the triple-reggeon RRP graph. From data presented in Ref [15], where the η-meson production by π^+- and π^--mesons on hydrogen at 100 Gev/c has been studied, we can conclude that in the

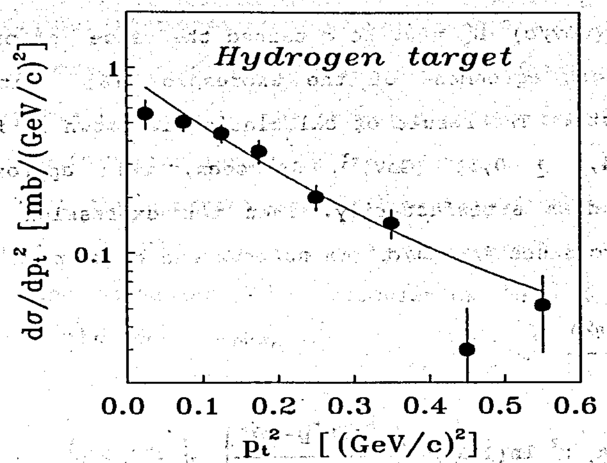

Fig.10. Differential cross section $d\sigma/dp_t^2$ for production of η-meson on hydrogen. The curve is the result of approximation formula (8)

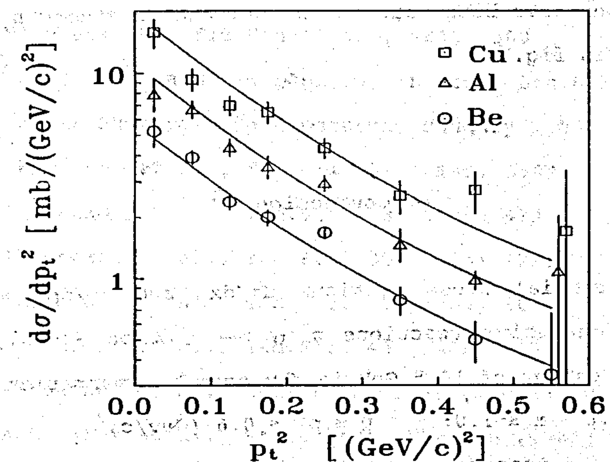

Fig.11. Differential cross sections $d\sigma/dp_t^2$ for process $\pi^+ + A \longrightarrow \eta + X$ on the targets Be,Al,Cu. The curve is the result of calculation by formula (9)

region $|t| \le 1$ $(\mathrm{GeV}/c)^2$ $B_P^\circ = 0$. We obtained the value of parameter B_R° from the best agreement of the expression (8) with the experimental data. The result of calculation is shown in fig. 10, here $B_R^\circ = (4{,}8 \pm 0{,}5)$ $(\mathrm{GeV})^{-2}$. As seen, this approximation describes the data satisfactorily. Then the expression for the differential cross section $d\sigma/dp_t^2$ on nucleus can be written as

$$\frac{d\sigma(\pi^+A \longrightarrow \eta X)}{dp_t^2} =$$

$$\int B_P \cdot \exp(2\alpha'_{A_2} p_t^2 \ln(1-x_F)) \cdot \left(\frac{d\sigma(\pi^+p\to\eta X)}{dx_F}\right)_P \cdot \left(A_{eff}^A(x_F)\right)_P + \qquad (9)$$

$$\exp(-B_R^\circ p_t^2) \int B_R \cdot \exp(2\alpha'_{A_2} p_t^2 \ln(1-x_F)) \left(\frac{d\sigma(\pi^+p\to\eta X)}{dx_F}\right)_R \cdot \left(A_{eff}^A(x_F)\right)_R,$$

The calculations have been made for Be, Al and Cu. targets. Results are presented in fig.11.

4. Conclusion

The differential cross sections $d\sigma/dx_F$ and $d\sigma/dp_t^2$ have been measured for inclusive reactions $\pi^- + A \longrightarrow \eta X$ on H,D,Li,Be,Al,Cu nuclei at the energy of 10.5 GeV in the beam fragmentation region:

$$0.6 \le x_F \le 1.0; \qquad 0 \le p_t^2 \le 0.6 \ (\mathrm{GeV}/c)^2.$$

The fragmentation process $\pi \longrightarrow \eta$ was described within the framework of the model[11] which allows for colour transparency of nuclei and effects of final state formation length . Taking into account the QCD-predicted dependence of the interaction cross section on the quark structure of hadrons (colour screening) one can qualitatively describe experimental data for a large group of targets. Because of relatively small energy of the beam (10.5 GeV) the momentum dependence on the formation length is insignificant.

Note that the approach used in this paper for description of p_t^2-dependence of differential cross sections is too simplified, because the mechanism for calculation of $d\sigma/dp_t^2$ is not developed in the model used.

References

[1] Yu.P.Nikitin, I.L.Rosental High Energy Nuclear Physics, (Moscow, 1980)
N.N.Nikolaev, Usp.Fiz.Nauk 134 (1981) 369
B.Z.Kopeliovich and L.I.Lapidus, in Proc. 6th Balaton Conf. on Nuclear Physics (Balatonfured, Hungary 1983) p.169

[2] S.A.Akimenko et al., Yad.Fiz. 52 (1990) 1397
S.A.Akimenko et al., Yad.Fiz. 53 (1990) 429

[3] S.A.Akimenko et al., Yad.Fiz. 38 (1983) 1212
S.A.Akimenko et al., Yad.Fiz. 39 (1984) 649

[4] S.A.Akimenko et al., Yad.Fiz. 43 (1986) 615

[5] G.S.Bitsadze et al., Nucl.Phys. B279 (1987) 770

[6] V.A.Antyukhov et al., Prib. Tekh. Eksp. 5 (1985) 35

[7] G.S.Bitsadze et al., Prib. Tekh. Eksp. 4 (1987) 52

[8] G.S.Bitsadze et al., Phys. Lett. 167B (1986) 138

[9] S.N.Malyukov et al., JINR Report P10-86-138, Dubna (1986)

[10] James F.and Roos M., Comp. Phys. Comm. 10 (1975) 343

[11] Kopeliovich B.Z., Litov L.B., Nemchik J., JINR Preprint E2-90-344 Dubna (1990)

[12] B.Z.Kopeliovich, N.A.Russakovich, JINR Preprint E2-86-298 Dubna (1986) (submitted to XXIII Int.Conf. on High Energy Physics (Berkeley, USA, 1986))

[13] A.B.Kaidalov, Phys. Lett. B116 (1982) 459
A.B.Kaidalov, K.A.Ter-Martirosyan, Phys. Lett. B117 (1982) 247
A.B.Kaidalov, K.A.Ter-Martirosyan, Yad.Fiz. 39 (1984) 154
A.B.Kaidalov, Yad.Fiz. 45 (1987) 1452

[14] B.Z.Kopeliovich, JINR Preprint P2-84-698 Dubna (1984)

[15] Barnes A.V. et al., Nucl.Phys. B145 (1978) 45

Received by Publishing Department
on Novemder 14,1991.